PCCP

Accepted Manuscript

ROYAL SOCIETY OF CHEMISTRY

www.rsc.org/pccp

Acetylene as an Essential Building Block for Prebiotic Formation of Pyrimidine Bases on Titan

Yassin A. Jeilani,[a,*] Chelesa Fearce,[a] Minh Tho Nguyen,[b]

[a] *Department Chemistry and Biochemistry, Spelman College, Spelman Lane, S.W., Box 1134, Atlanta, GA 30314, USA*

[b] *Department of Chemistry, University of Leuven, B-3001 Leuven, Belgium*

(*) E-mail: yjeilani@spelman.edu, Tel: 404-270-5746

ABSTRACT

Prebiotic building blocks for the formation of biomolecules are important in understanding the abiotic origin of biomolecules. However, there is a limited choice of the building blocks as precursors for the biomolecules. Acetylene (HCCH) is found in Titan's atmosphere and is an abiotic-precursor of pyrimidine bases. HCCH reacts with urea to form both cytosine and uracil. The mechanisms for the formation of both cytosine and uracil were studied by density functional theory at B3LYP/6-311G(d,p). Ethynyl radicals (•CCH) are relevant for the chemistry of Titan's atmosphere therefore both HCCH and •CCH were evaluated as carbon sources. The pathways, for both HCCH and •CCH, lead to intermediates with an unsaturated-group that facilitate the formation of the six-membered ring of the pyrimidine bases. The predicted structures for cytosine and uracil were compared with labeled cytosine and uracil that were formed from the reaction of DCCD with urea. The results suggest that cytosine is formed from HCCH while uracil is formed from •CCH. The mechanisms are energetically feasible and there is no conclusive evidence for the preferred pathway (HCCH or •CCH). The pathways were further extended for the formation of both uric acid and 8-oxoguanine from HCCH and urea, demonstrating the utility of HCCH as a carbon source for diverse biomolecules. Biuret is identified as a precursor for the pyridimine bases, and it unifies the free radical pathways for the pyrimidine bases with those of triazines. The pathways are appropriate for the reducing atmosphere that creates both radicals and electrons due to ionizing radiation on Titan. The mechanisms are feasible for the extraterrestrial formation of the pyrimidine bases.

KEYWORDS: Prebiotic formation of pyrimidine bases, cytosine, uracil, Titan, free radicals.

I. Introduction

Acetylene (HCCH) has been observed on Titan,[1] cometary comae,[2] interstellar molecular clouds,[3] and protoplanetary disks.[4] HCCH has been used in laboratory experiments for the simulation of Titan's aerosols.[5] It is an important source of carbon for the formation of organic compounds. HCCH together with urea has been used as carbon-source in simulated prebiotic reactions. Pyrimidine bases, along with other biomolecules, are formed under these conditions. The pathways for these reactions are complex and involve free radicals.

Interestingly, acetylene radical cations also react with HCN to form pyrimidine cations.[6] Ethynyl radical (•CCH) has been reported as a good source of carbon for reactions taking place in Titan's atmosphere. This radical (•CCH) is produced in the photolysis reactions of acetylene.[7–9] Previous studies on the reaction mechanisms have focused on •CCH as the building block for polyaromatic hydrocarbons.[10] Combined cross beam experiments and computations demonstrated that the reactions of •CCH proceed through radical addition reactions to unsaturated bonds (double and triple bonds). These reactions are important in understanding the photochemistry on the planetary atmospheres.[11]

Sagan and Thompson suggested that organic compounds can also be formed by condensed ices under conditions relevant to Titan's atmosphere.[11] In a simulation experiment of Titan's atmosphere, Hörst *et al.* reported formation of nucleobases including cytosine and uracil together with other compounds.[12] These compounds constitute Titan's haze, which is a good source of prebiotic compounds.[13]

Tholins are also good sources of prebiotic precursors such as urea. Urea is formed in electric discharge experiments after acid hydrolysis of the resulting tholins at high-temperature.[14] Urea was also formed when laboratory ice analogs of Titan's aerosols were irradiated with cold

plasma discharge.[15] In addition, cytosine and uracil have been detected in the hydrolysis products of tholins at low temperatures.[16] Acid hydrolysis of HCN oligomers led to the release of uracil.[17] Tholins are complex mixtures of organic compounds that provide prebiotic precursors to biomolecules.

Nucleobases such as purines have also been detected in meteorites.[18] Uracil was found in Murchison, Murray, and Orgueil carbonaceous meteorites.[19] Ehrenfreund and Charnley suggested that meteoritic impacts on early Earth could have delivered the biomolecules in large amounts.[20] The extraterrestrial origin of the biomolecules has also been suggested.

Reactions taking place on Titan are initiated mainly by ultraviolet light (UV) from the sun, Saturn's magnetosphere electrons or protons, cosmic rays, or interplanetary electrons.[11] Free radical pathways are appropriate for these reactions, which can produce a range of organic aerosols with nitrogen content. Rica *et al.* reported mechanisms for the incorporation of nitrogen into an aromatic ring using density functional theory (DFT).[21] Mechanisms involving carbenes lead to cytosine and uracil but the pathways have high energy barriers.[22] Understanding the prebiotic mechanisms to incorporate nitrogen into aerosol compounds (tholins) for the formation of biologically relevant molecules such as nucleobases remains a challenging problem and these mechanisms are not yet well established.

Pyrimidine bases and triazines are formed in spark-discharge experiments of urea in $CH_4/N_2/H_2$.[23] When urea is sparked under argon, triazines are formed without the pyrimidine bases. We reported the free radical mechanisms for these reactions (Scheme 1).[24] To further probe the prebiotic building blocks for diverse biomolecules, the reactions were performed with urea and HCCH as carbon sources.[25] These experiments led to the formation of both triazines and pyrimidine bases. Therefore the mechanisms, in the current study, for the formation of

pyrimidine bases are unified with those of triazines (Scheme 1). HCCH reacts through addition reactions to the triple bond or through the generation of •CCH, therefore, the pathways of HCCH are compared with those of •CCH. These pathways are essential in addressing the long-standing challenge in finding the prebiotic building blocks for biomolecules.

II. Computational Methods

All standard calculations using density functional theory (DFT) was performed with the aid of the Gaussian 09 suite of programs.[26] The hybrid B3LYP functional,[27,28] in conjunction with the 6-311G(d,p) basis set was used for all calculations.[29] Harmonic vibrational frequency calculations were carried out at the same level in order to confirm the nature of stationary points, and to obtain zero-point vibrational energies. Each transition structure was characterized by having one imaginary vibrational frequency for the normal mode corresponding to the correct reaction coordinate. Intrinsic reaction coordinate (IRC) calculations at B3LYP/6-311G(d,p) level of theory were performed to confirm the connections between all saddle points and respective minima.[30,31] Geometrical parameters of the relevant stationary points are listed in the Supplementary Information file. The popular B3LYP functional has been employed in several previous studies to explore the production of purine nucleobases in both neutral and free radical states under prebiotic conditions.[32–35] Vibrational frequency analyses were carried out at the same level of theory to obtain the zero-point correction energy (ZPE) and to confirm the nature of each stationary point. A uniform scaling factor of 0.967 was used for the ZPE values when calculating the relative energies of the structures considered. Computational resources (XSEDE)[36] available at Gridchem website (http:www.gridchem.org) were used to perform the calculations.[37,38]

III. Results and Discussions

The mechanisms in this study are based on the prebiotic scenario proposed by Menor-Salván *et al.* in which eutectic water/ice/urea is irradiated with UV light (254 nm) under HCCH gas.[25] In this scenario, both HCCH and urea are used as sources of carbon for the formation of the pyrimidine bases in free radical pathways. It is a general principle in free radical chemistry that the reactions can lead to more than one pathway and, in many cases, this is the limiting factor of free radicals in traditional chemistry. However, once the reaction is initiated, free radicals are reactive species that can account for the abiotic formation of diverse biomolecules. The current study suggests that cytosine and uracil also generate reactive species through free radical pathways to form both uric acid and 8-oxoguanine.

The first step of the mechanism is the formation of radical **2** from urea (**1**) followed by the addition of **2** to a second urea molecule to give biuret (**4**) with the elimination of an $\bullet NH_2$ (Scheme 2). These steps lead to **4** as a precursor for both cytosine and uracil. The first sequence of steps, **1** → **2** → **3** → biuret (**4**), are the same as previously described for the formation of cyanuric acid (Scheme 1).[24]

1. Formation of Cytosine

Biuret (**4**) is a versatile precursor because it has two equivalent carbonyl groups and two NH_2 groups that can participate in radical reactions. Two possible routes for the formation of cytosine are the reaction of **4** with either HCCH or •CCH. Scheme 2 shows the addition reactions of both HCCH and •CCH with biuret. These additions are followed by a six-membered ring cyclization. The main difference in these routes is that the cyclization involves a triple bond or a

double bond for the •CCH or HCCH cases, respectively. Figure 1 and 2 show the potential energy diagrams, respectively, for these two routes leading to cytosine.

Addition of HCCH to biuret (**4**) takes place in two steps. The first step is a hydrogen abstraction step followed by an addition to the triple bond of HCCH. These two steps (**4** → **5a** → **6a**) are both exergonic with small energy barriers of 3.9-6.9 kcal/mol (Figure 1). The energy release in the step **5a** → **6a** can be attributed to the conversion of the triple bond of HCCH to a double bond. This energy is available for the energy demanding steps of the pathway. The structure of **6a** has all atoms required for the formation of cytosine. The vinyl radical in **6a**, originating from the HCCH, adds to the C=O group to form the six-membered ring radical **7a**. This intramolecular radical attack has an energy barrier of 23.8 kcal/mol.

Formation of cytosine from **8a** requires the elimination of an OH group. Therefore a 1,3-hydrogen rearrangement (**7a** → **8a**) takes place first to allow this elimination. The energy barrier ($\Delta E^{\#}$: 32.1 kcal/mol) for this step is the highest along the HCCH pathway. Elimination of an •OH from **8a** completes the path to cytosine (**9a**). Scheme 2 shows that all carbons and hydrogens from HCCH are retained in cytosine.

Turning now to the ethynyl radical (•CCH) route, addition of •CCH to the carbonyl group of biuret (**4**) gives **5b** with the release of 12.8 kcal and a small energy barrier of 1.4 kcal/mol. The next step is the elimination of •OH group that takes place in two steps which is analogous to the HCCH pathway. The elimination of the •OH is preceded by a 1,3-hydrogen rearrangement step. Similar to the HCCH pathway, the rearrangement step (**5b** → **6b**) has the highest energy barrier ($\Delta E^{\#}$: 26.2 kcal/mol). The •OH elimination from **6b** gives the neutral intermediate **7b** that can be activated with an $•NH_2$. Subsequent hydrogen abstraction from **7b** gives the radical molecule complex **8b**.

The cyclization of **8b** is achieved by an intramolecular radical attack on the triple bond to form the six-membered ring within the complex **8b**. This radical attack on the triple bond is the main difference from the HCCH pathway where a vinyl radical is involved in the cyclization to form the six-membered ring. This difference is reflected in the release of 34.3 kcal/mol for the cyclization **8b** → **9b** versus the endothermic (ΔE: 7.4 kcal/mol) cyclization **6a** → **7a**. Hydrogen abstraction by the resulting vinyl radical, **9b** → cytosine (**9a**), is again exothermic and almost barrierless ($\Delta E^{\#}$: 0.1 kcal/mol). Finally, Figure 1 shows that formation of cytosine via •CCH pathway is associated with a release of 43.7 kcal/mol while the HCCH route leads to cytosine with the release of 10.8 kcal/mol. The energetically favored •CCH pathways can be attributed to the release of energy associated with •CCH addition (**4** → **5b**), cyclization (**7b** → **8b**), and vinyl radical hydrogen abstraction (**9b** → **9a**).

2. Formation of Uracil

Uracil is the pyrimidine base required for ribonucleic acid (RNA). The main difference between cytosine and uracil is the substitution of C4. The HCCH pathway for uracil is essentially the same as that for cytosine with the exception of the last elimination step taking place from **7a**. The intermediate **7a** (Scheme 2), along the cytosine pathway, has all atoms needed for the formation of uracil with the correct connectivity. Therefore, the elimination process at C4 determines if the product is cytosine or uracil.

The radical induced elimination of $\bullet NH_2$ from **7a** leads to uracil (**10a**) while cytosine formation from **7a** requires a hydrogen rearrangement as explained above. The elimination of $\bullet NH_2$, **7a** → **10a**, is exergonic (ΔE: - 11.7 kcal/mol) with an energy barrier of 4.0 kcal/mol. The structure of uracil from this route retains all atoms from HCCH.

The •CCH pathway to produce uracil proceeds through low energy barriers (Figure 3). The elimination of an •NH_2 group from the addition product **5b** leads to **11** (Scheme 3) with a small energy barrier of 4.8 kcal/mol. Similar to the •CCH pathway for cytosine, the final three steps are hydrogen abstraction **11** → **12**, addition to triple bond **12** → **13** and hydrogen abstraction **13-NH_2** → **10a** by the vinyl carbon. The last two steps are exergonic with a net release of 52.8 kcal/mol (Figure 3). All atoms in •CCH are part of the ring framework in uracil (Scheme 3).

3. Formation of Uric Acid

Uric acid is a known scavenger in biological systems. It protects nucleobases (including uracil) from ozone induced degradation.[39] It has good scavenging activities for •OH.[40] Simic and Jovanovic suggested that uric acid may act as a repair agent of oxidative damage to nucleobases.[41] These scavenging properties of uric acid can also protect pyrimidine bases from the ionizing irradiation in planetary environment that generate electrons and free radicals. Currently, there are no studies on the prebiotic scavenging activities of uric acid. Nevertheless, a possible role of uric acid as a defense system for the newly synthesized pyrimidine bases is an attractive prebiotic scenario which may be important for the accumulation of the pyrimidine bases. Uric acid was also formed together with cytosine and uracil under the aforementioned eutectic water/ice/urea experiment.[25]

The intermediate **24** (Scheme 4) is precursor for both uric acid (Scheme 5) and 8-oxoguanine (Scheme 5). The pathway is initiated by the addition of **2** to the triple bond of HCCH leading to the vinyl radical **14**. Similar to the pathways for pyrimidine bases, this addition is highly exergonic with the release of 24.5 kcal/mol. The resulting radical **14** forms a radical

molecule complex **15**. The vinyl radical within the complex **15** abstracts a hydrogen from NH_3 forming $\bullet NH_2$. Another hydrogen abstraction by this radical leads to **17** with an energy barrier of 9.1 kcal/mol that is slightly higher that the hydrogen abstraction taking place in the radical molecule complex step **15** → **16** (Figure 4). The cyclization step **17** → **18** leads to the five membered ring of uric acid. Two more urea molecules are required for the formation of uric acid. The addition of the carbon radical **18** to the carbonyl group of urea has a much higher energy barrier ($\Delta E^{\#}$: 30.9 kcal/mol) than the addition of the acetylene radical **4** → **5b** ($\Delta E^{\#}$: 1.4 kcal/mol).

Next, the hydrogen abstraction step **20** → **21** is required for the formation of the double bond in **22**. The bottleneck for the formation of the double bond is the loss of an H radical from **21** that has a barrier of 30.2 kcal/mol. Similar to **18** → **19**, the addition of the nitrogen radical to the carbonyl of urea (**23** to **24**) has a higher energy barrier than the addition of •CCH to the carbonyl group (Figure 4). This demonstrates the advantage of the •CCH in addition reactions that is associated with rather small barrier. The hydrogen abstraction steps (**15** → **16**, **16** → **17**, **20** → **21**, and **22** → **23**) have small energy barriers along the pathway for the formation of **24**.

The radical **24** leads to uric acid in four steps (Scheme 4) and the loss of an H radical has the highest energy barrier (Figure 5). The initial loss of $\bullet NH_2$ from **24** is exergonic with the release of 18.8 kcal/mol and this is similar to the loss of $\bullet NH_2$ in **7a** → **10a** step; the energy released in this step could be available for next energy demanding steps. Hydrogen abstraction within the radical molecule complex **25** is followed by the loss of an H radical to give uric acid (**28**). The energy barrier ($\Delta E^{\#}$: 36.4 kcal/mol) for **27** → **28** is higher than the H radical loss in **21** → **22** ($\Delta E^{\#}$: 30.2 kcal/mol). The net energy release from **2** to **24**, and, from **24** to **28** is relatively

less than the energy released from the formation of cytosine (**9a**) and uracil (**9a**) as shown in Figures 1, 3-5.

4. Formation of 8-Oxoguanine

In biochemical systems, 8-oxo-7,8-dihydroguanine (8-oxoguanine) is a known endogenous mutagen. It forms base-mismatch with adenine in deoxyribonucleic acid (DNA).[42] In prebiotic reactions, 8-oxoguanine is another product of eutectic water/ice/urea experiments with the pyrimidine bases.[25] It has structural similarities with uric acid, therefore, the intermediate **24** also leads to 8-oxoguanine (Scheme 5). The possibility to synthesize more known biomolecules from the same precursors is an advantage of free radical mechanisms.

Although **24** leads to uric acid and 8-oxoguanine (Scheme 5), the pathway for the 8-oxoguanine (**36**) is more energy demanding than the uric acid (**28**) path (Figure 6). In addition, the hydrogen rearrangement **32** → **33** and loss of hydrogen radical **33** → **34** have the highest energy barriers (Figure 6). For the hydrogen rearrangement, it requires smaller barrier when the 1,3-hydrogen rearrangement takes place with heteroatoms **24** → **29** ($\Delta E^{\#}$: 27.4 kcal/mol) than the 1,2-hydrogen rearrangement **32** → **33** ($\Delta E^{\#}$: 47.2 kcal/mol) at the bridgehead carbons. These barriers are prohibitively high for this pathway to proceed unless there is some kind of catalysis by the ice involved in the pathway. The reactions were indeed performed in a freeze-thaw cycle and it is not clear if ice played a role in lowering the energy barriers under these conditions. However, previous studies have suggested that water-ice can play a catalytic role in heterogeneous reactions under presumed prebiotic conditions.[43,44] Also, ultraviolet (UV) irradiation has been often used to induce formation of radicals. In addition to the ground state calculations in the current study, UV irradiation may generate excited states and alternative

pathways with low-energy barriers are possible. Nevertheless, the current study provides the first computational evidence that 8-oxoguanine can be formed from urea and acetylene.

The loss of •OH leading to **30** is followed by hydrogen abstraction **30** → **31** that has low energy barrier (Figure 6). The energy release of 15.5 kcal/mol in the cyclization step **31** → **32** is less than the energy released from the cyclization steps involving a triple bond in the **8b** → **9b** and **12** → **13** steps (34.3-36.2 kcal/mol). Note these cyclization steps involve the net break of one π-bond and the formation of one σ-bond; the double bond releases about half the energy released from the triple bond in these transformations. The next two steps, hydrogen rearrangement **32** → **33** and loss of hydrogen **33** → **34**, have the highest barrier in this pathway. Figure 5 shows an energy releasing step **34-NH_2** → **35** immediately after these two steps is followed by hydrogen abstraction to give 8-oxoguanine (**36**).

5. Importance of Temperature on the Pathways

The reactions of the proposed pathways have been reported at low temperature; therefore the effects of lowering the temperature on the pathways were evaluated in terms of enthapy barriers, enthalpy of reactions, Gibbs free energy barriers, and Gibbs free energies of reactions at the surface temperature of Titan (94 K), temperature of ice (273 K), and the standard ambient temperature (298 K). Figure 7 shows the energy, enthalpy and Gibbs free energy profiles in black, red, and blue, respectively, for both HCCH and •CCH routes. There are significant temperature effects on the Gibbs free energy profile while the enthalpy profile correlates well with the energy profiles at all temperatures. A slight decrease in temperature from 298 K to 273 K does not have a major impact on the pathways. These results suggest that the decrease in the entropy factor of the Gibbs free energy as the temperatue decreases favors the pathways at the

surface temperature of Titan. This suggests that the formation of the nucleobases is energetically could be favored on the surface of Titan.

6. Prebiotic Implications of the Pathways

The mechanisms presented here for the four biomolecules complement the previous pathways for the formation of triazines (melamine, ammeline, ammelide and cyanuric acid) using urea as a source of C, N, O, and H under similar simulated planetary conditions.[24] Pathways involving urea could be important for HCN pathways because cytosine is detected in the hydrolysis products of HCN polymers. Urea has also been detected in the mixture resulting from heating HCN polymers.[45] The mechanisms provide a fundamental insight on the abiotic origin of the pyrimidine bases with greater emphasis on the fixed nitrogen in the form of nitrogenous organic compounds, *i.e.*, biomolecules.

The key findings – pathways from acetylene to biomolecules – suggest that reactions of the ethynyl radical (•CCH) could be as important as addition reactions to the triple bond of HCCH in the planetary atmosphere. Scheme 6 shows the deuterated cytosine and uracil that were observed in experiments performed with DCCD.[25] Comparison for the location of the HCCH moiety in the predicted structures of pyrimidine bases with the experimentally observed deuterated- cytosine and uracil suggests that cytosine is formed from HCCH while uracil is formed from •CCH. The DCCD provides two deuterium atoms to cytosine (Scheme 6) as predicted by the HCCH pathways. On the other hand, only one deuterium atom is incorporated into the correct position of uracil, as predicted by, the •CCH pathway. Uracil with two deuterium atoms was not been experimentally observed. However, bot mechanisms are energetically feasible, and there is no conclusive evidence for the preferred pathway (HCCH or •CCH).

Though the reactions on Titan are likely occurring even now, these pathways may provide new target compounds, especially the neutral intermediates, for future missions to Titan. It should also be clear from this discussion that the free radical mechanisms set no limitations on the number of products formed. This is consistent with reactions performed in the laboratory under presumed prebiotic conditions usually give a complex mixture of compounds. Even more important, the proposed mechanisms contribute to the understanding of the nitrogen fixation process and may be important for the formation of the brown haze on Titan.

IV. Conclussions

The mechanisms show that the pathways leading to cytosine and uracil are energetically feasible for the cold conditions on Titan's surface. The cyclization steps, **8b** → **9b** and **12** → **13**, of the •CCH pathways involve direct radical attack on the triple bond moiety, and both steps are exergonic with the release of 34.3 kcal/mol and 36.2 kcal/mol, respectively. The •CCH pathway allows the release of energy that is stored in the triple bond during the cyclization efficiently. The results suggest that HCCH serves as a carbon source and an energy source in prebiotic reactions.

The mechanisms include the following steps associated with the formation of the selected compounds: (a) losses of $\bullet NH_2$ (**7a** → **10a**, **24** → **25**), (b) hydrogen abstractions (**15** → **16**, **16** → **17**, **20** → **21**, **22** → **23**, and **30** → **31**), (c) hydrogen rearrangements (**5b** → **6b**, **7a** → **8a**, **21** → **22**, and **24** → **29**), and (d) hydrogen radical losses (**27** → **28, 21** → **22,** and **33** → **34**). As expected, the hydrogen abstractions had relatively low energy barriers; DFT methods and other GGA functionals are known to underestimate these barriers up to 10 kcal/mol and a calibration has been previously reported.[46]

Acknowledgements

Both YJ and CF are thankful to the generous support by the Research Initiative for Scientific Enhancement program (Grant # 2R5GM06566-13). GridChem (http:www.gridchem.org) is acknowledged for computational resources and services that were used to perform the DFT studies. This work used the Extreme Science and Engineering Discovery Environment (XSEDE), which is supported by National Science Foundation grant number ACI-1053575.

References

1 R. K. Khanna, *Icarus*, 2005, **178**, 165–170.

2 M. J. Mumma, M. A. DiSanti, N. D. Russo, K. Magee-Sauer, E. Gibb and R. Novak, *Adv. Space Res.*, 2003, **31**, 2563–2575.

3 J. H. Lacy, N. J. Evans, J. M. Achtermann, D. E. Bruce, J. F. Arens and J. S. Carr, *Astrophys. J.*, 1989, **342**, L43–L46.

4 M. Agúndez, J. Cernicharo and J. R. Goicoechea, *Astron. & Astrophys.*, 2008, **483**, 831–837.

5 T. W. Scattergood, E. Y. Lau and B. M. Stone, *Icarus*, 1992, **99**, 98–105.

6 A. M. Hamid, P. P. Bera, T. J. Lee, S. G. Aziz, A. O. Alyoubi and M. S. El-Shall, *J. Phys. Chem. Lett.*, 2014, **5**, 3392–3398.

7 J. O. P. Pedersen, B. J. Opansky and S. R. Leone, *J. Phys. Chem.*, 1993, **97**, 6822–6829.

8 J. E. Murphy, A. B. Vakhtin and S. R. Leone, *Icarus*, 2003, **163**, 175–181.

9 R. J. Hoobler and S. R. Leone, *J. Geophys. Res. Planets*, 1997, **102**, 28717–28723.

10 A. M. Mebel, V. V. Kislov and R. I. Kaiser, *J. Am. Chem. Soc.*, 2008, **130**, 13618–13629.

11 C. Sagan and W. R. Thompson, *Icarus*, 1984, **59**, 133–161.

12 S. M. Hörst, R. V. Yelle, A. Buch, N. Carrasco, G. Cernogora, O. Dutuit, E. Quirico, E. Sciamma-O'Brien, M. A. Smith and Á. Somogyi, *Astrobiology*, 2012, **12**, 809–817.

13 C. K. Materese, M. Nuevo, P. P. Bera, T. J. Lee and S. A. Sandford, *Astrobiology*, 2013, **13**, 948–962.

14 B. N. Khare, C. Sagan, H. Ogino, B. Nagy, C. Er, K. H. Schram and E. T. Arakawa, *Icarus*, 1986, **68**, 176–184.

15 S. I. Ramírez, P. Coll, A. Buch, C. Brassé, O. Poch and F. Raulin, *Faraday Discuss.*, 2010, **147**, 419–427.

16 C. D. Neish, Á. Somogyi and M. A. Smith, *Astrobiology*, 2010, **10**, 337–347.

17 A. B. Voet and A. W. Schwartz, *Orig. life*, 1982, **12**, 45–49.

18 M. P. Callahan, K. E. Smith, H. J. Cleaves, J. Ruzicka, J. C. Stern, D. P. Glavin, C. H. House and J. P. Dworkin, *Proc. Natl. Acad. Sci.*, 2011.

19 P. G. Stoks and A. W. Schwartz, 1979.

20 P. Ehrenfreund and S. B. Charnley, *Annu. Rev. Astron. Astrophys.*, 2000, **38**, 427–483.

21 A. Ricca, C. W. Bauschlicher and E. L. O. Bakes, *Icarus*, 2001, **154**, 516–521.

22 T. Wang and J. H. Bowie, *Org. & Biomol. Chem.*, 2012, **10**, 652–662.

23 C. Menor-Salván, D. Ruiz-Bermejo, M. I. Guzmán, S. Osuna-Esteban and S. Veintemillas-Verdaguer, *Chem. Eur. J.*, 2009, **15**, 4411–4418.

24 Y. A. Jeilani, T. M. Orlando, A. Pope, C. Pirim and M. T. Nguyen, *RSC Adv.*, 2014, **4**, 32375–32382.

25 C. Menor-Salván and M. R. Marín-Yaseli, *Chem. Eur. J.*, 2013, **19**, 6488–6497.

26 M. J. Frisch, G. W. Trucks, H. B. Schlegel, G. E. Scuseria, M. A. Robb, J. R. Cheeseman, G.

Scalmani, V. Barone, B. Mennucci and G. A. Petersson, *Gaussian Inc., Wallingford*, 2009.

27 A. D. Becke, *Phys. Rev.*, 1988, **38**.

28 C. Lee, W. Yang and R. G. Parr, *Phys. Rev. B*, 1988, **37**.

29 W. J. Hehre, L. Radom, P. von R. Schleyer and J. A. Pople, *Ab initio molecular orbital theory*, Wiley New York et al., 1986, vol. 67.

30 H. P. Hratchian and H. B. Schlegel, *J. Chem. Phys.*, 2004, **120**, 9918–9924.

31 H. P. Hratchian and H. B. Schlegel, *J. Chem. Theory Comput.*, 2005, **1**, 61–69.

32 Y. A. Jeilani, H. T. Nguyen, D. Newallo, J.-M. D. Dimandja and M. T. Nguyen, *Phys. Chem. Chem. Phys.*, 2013, **15**, 21084–21093.

33 Y. A. Jeilani, H. T. Nguyen, B. H. Cardelino and M. T. Nguyen, *Chem. Phys. Lett.*, 2014, **598**.

34 D. Roy, K. Najafian and P. von Ragué Schleyer, *Proc. Natl. Acad. Sci.*, 2007, **104**, 17272–17277.

35 J. Wang, J. Gu, M. T. Nguyen, G. Springsteen and J. Leszczynski, *J. Phys. Chem. B*, 2013, **117**, 9333–9342.

36 J. Towns, T. Cockerill, M. Dahan, I. Foster, K. Gaither, A. Grimshaw, V. Hazlewood, S. Lathrop, D. Lifka and G. D. Peterson, *Comput. Sci. & Eng.*, 2014, **16**, 62–74.

37 N. Shen, Y. Fan and S. Pamidighantam, *J. Comput. Sci.*, 2014, **5**, 576–589.

38 R. Dooley, K. Milfeld, C. Guiang, S. Pamidighantam and G. Allen, *J. Grid Comput.*, 2006, **4**, 195–208.

39 J. Meadows and R. C. Smith, *Arch. Biochem. Biophys.*, 1986, **246**, 838–845.

40 J. R. León-Carmona and A. Galano, *J. Phys. Chem. B*, 2011, **115**, 15430–15438.

41 M. G. Simic and S. V. Jovanovic, *J. Am. Chem. Soc.*, 1989, **111**, 5778–5782.

42 S. D. Bruner, D. P. Norman and G. L. Verdine, *Nature*, 2000, **403**, 859–866.

43 F. Duvernay, T. Chiavassa, F. Borget and J.-P. Aycard, *J. Am. Chem. Soc.*, 2004, **126**, 7772–7773.

44 P. De Marcellus, M. Bertrand, M. Nuevo, F. Westall and L. Le Sergeant d'Hendecourt, *Astrobiology*, 2011, **11**, 847–854.

45 C. N. Matthews and R. D. Minard, *Faraday Discuss.*, 2006, **133**, 393–401.

46 M. T. Nguyen, S. Creve and L. G. Vanquickenborne, *J. Phys. Chem.*, 1996, **100**, 18422–18425.

Scheme and Figure Legends

Scheme 1. Pathways from urea to pyrimidine bases and triazines

Scheme 2. Mechanisms for the formation of cytosine and uracil. Red color is used for the acetylene moiety

Scheme 3. Mechanism for formation the formation of uracil from ethynyl radical. Red color is used for the acetylene moiety

Scheme 4. Mechanism for formation of precursor **24** for uric acid and 8-oxoguanine. Bold structure are used for the acetylene moiety

Scheme 5. Mechanism for formation of uric acid and 8-oxoguanine. Red color and bold structure are used for the acetylene moiety

Scheme 6. Deuterated cytosine and uracil formed from DCCD

Figure 1. Potential energy surface for formation of cytosine from HCCH. Relative energies are given in kcal/mol were obtained from B3LYP/6-311G(d,p) + ZPE computations

Figure 2. Potential energy surface for formation of cytosine from •CCH. Relative energies are given in kcal/mol were obtained from B3LYP/6-311G(d,p) + ZPE computations

Figure 3. Potential energy surface for formation of uracil from •CCH. Relative energies are given in kcal/mol were obtained from B3LYP/6-311G(d,p) + ZPE computations

Figure 4. Potential energy surface for formation of intermediated **24**. Relative energies are given in kcal/mol were obtained from B3LYP/6-311G(d,p) + ZPE computations

Figure 5. Potential energy surface for formation of uric acid. Relative energies are given in kcal/mol were obtained from B3LYP/6-311G(d,p) + ZPE computations

Figure 6. Potential energy surface for formation of 8-oxoguanine. Relative energies are given in kcal/mol were obtained from B3LYP/6-311G(d,p) + ZPE computations

Figure 7. Energy, enthalpy and Gibbs free energy profiles (black, red, and blue respectively) of the HCCH and •CCH routes leading to the formation of cytosine (**9a**) from formamide at 94 K, 273 K and 298 K. Relative energies are given in kcal/mol were obtained from B3LYP/6-311G(d,p) + ZPE computations

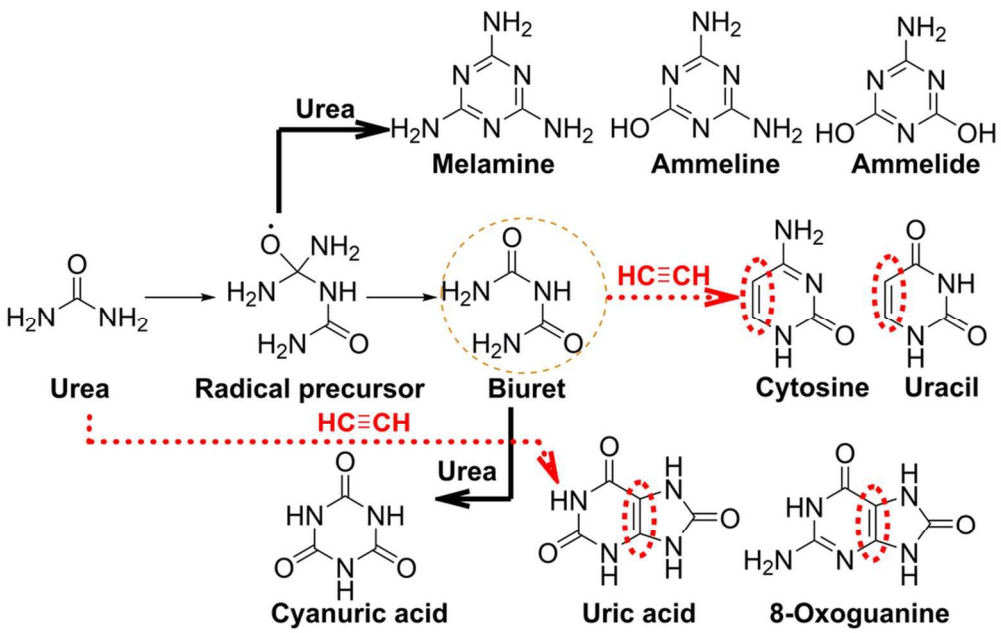

Scheme 1. Pathways from urea to pyrimidine bases and triazines
90x57mm (300 x 300 DPI)

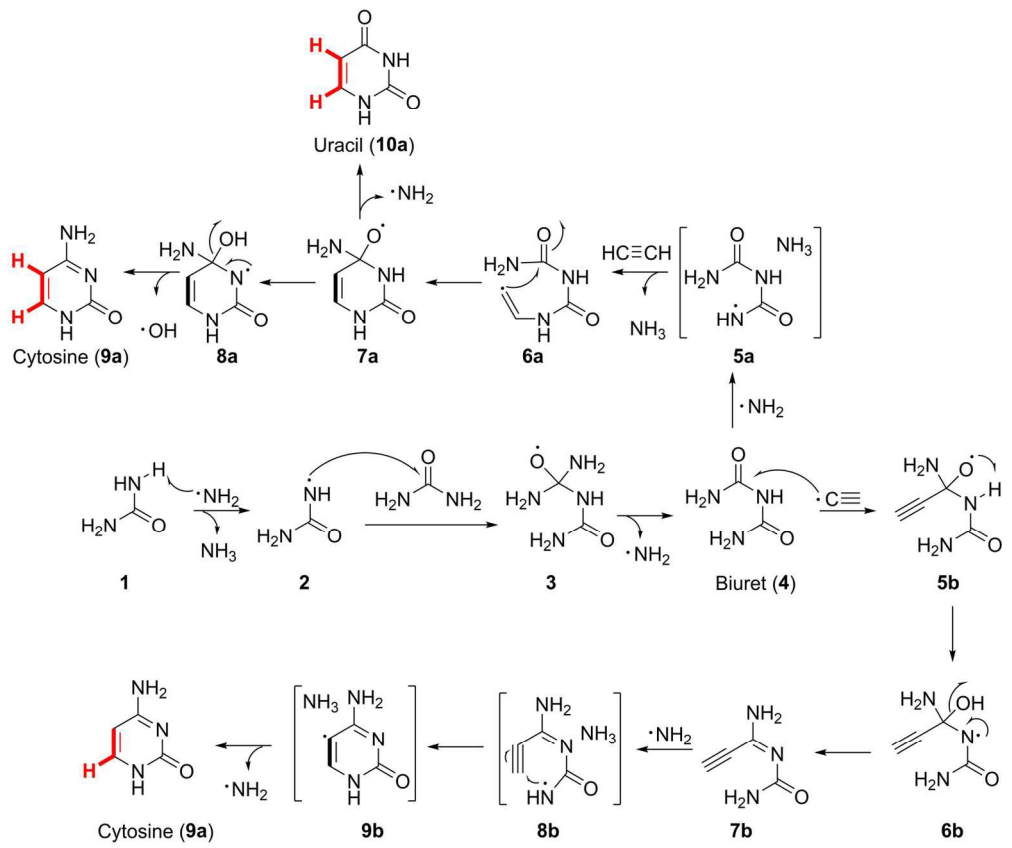

Scheme 2. Mechanisms for the formation of cytosine and uracil. Red color is used for the acetylene moiety
152x128mm (300 x 300 DPI)

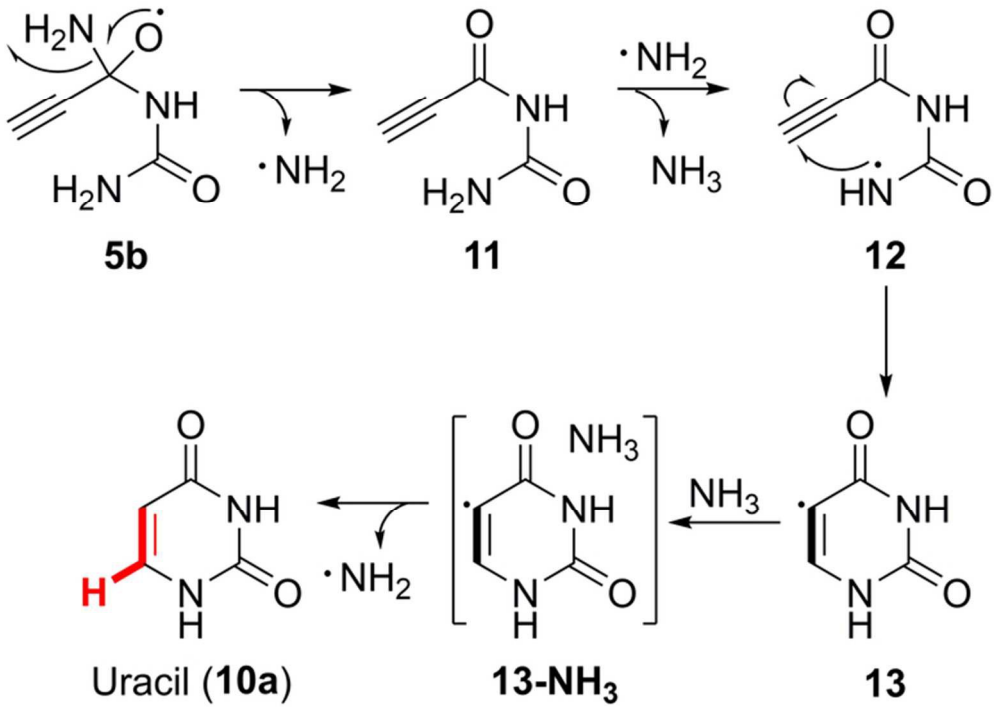

Scheme 3. Mechanism for formation the formation of uracil from ethynyl radical. Red color is used for the acetylene moiety
65x47mm (300 x 300 DPI)

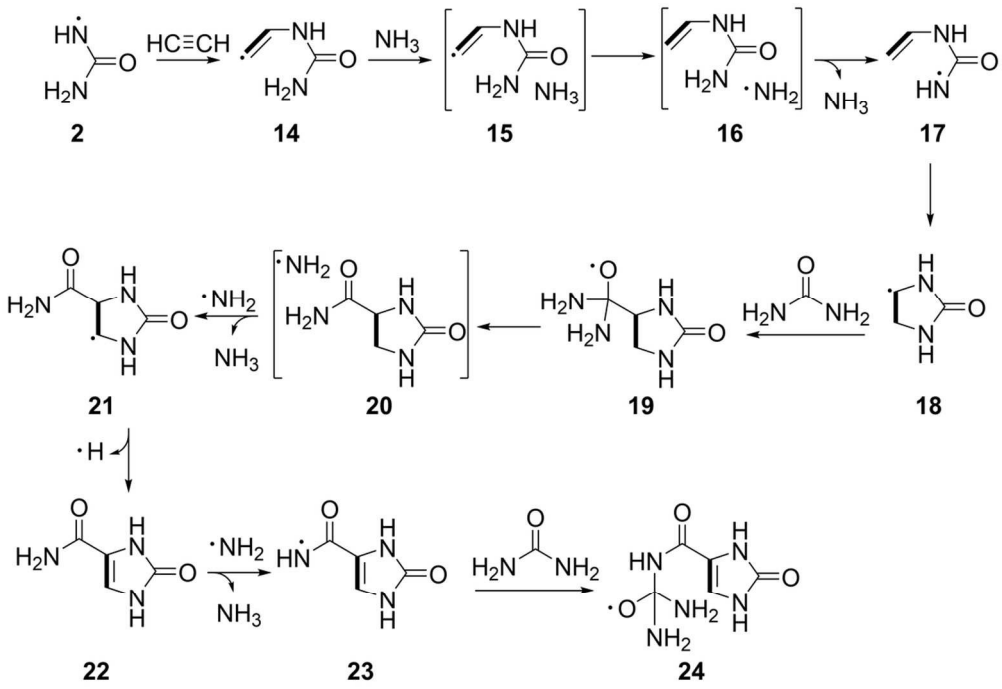

Scheme 4. Mechanism for formation of precursor 24 for uric acid and 8-oxoguanine. Bold structure are used for the acetylene moiety
109x75mm (300 x 300 DPI)

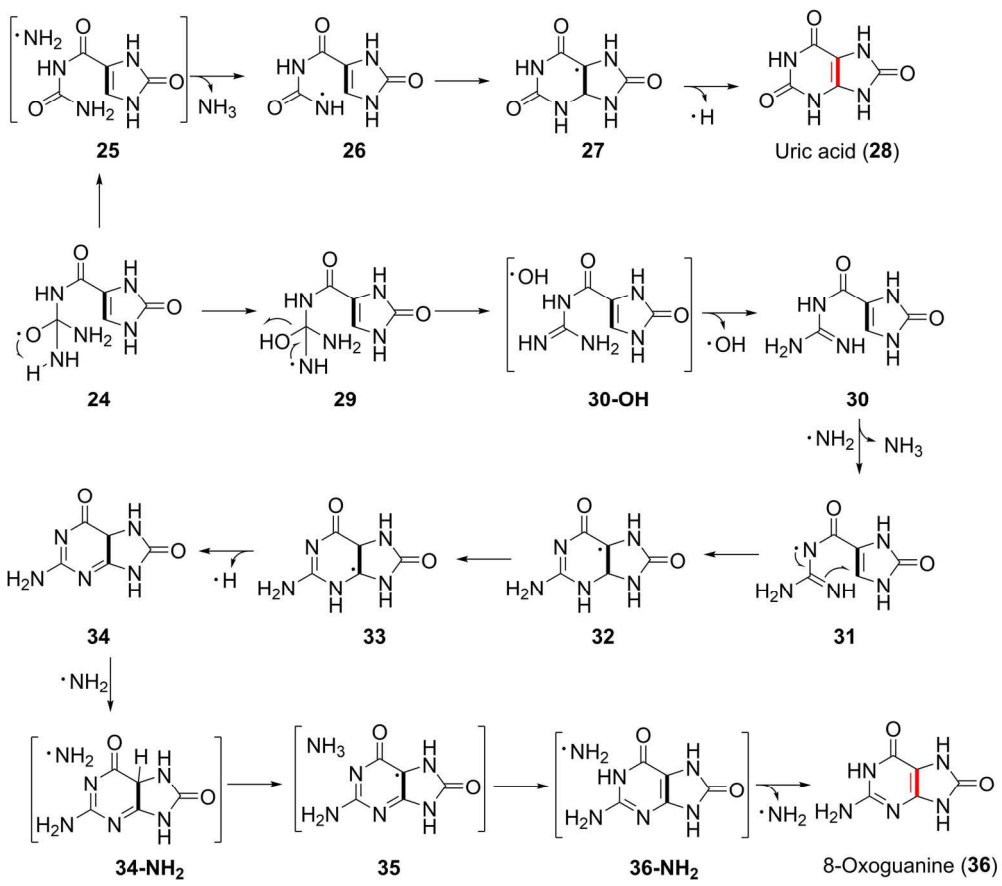

Scheme 5. Mechanism for formation of uric acid and 8-oxoguanine. Red color and bold structure are used for the acetylene moiety
162x143mm (300 x 300 DPI)

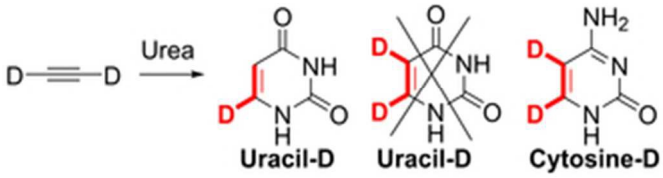

Scheme 6. Deuterated cytosine and uracil formed from DCCD
28x7mm (300 x 300 DPI)

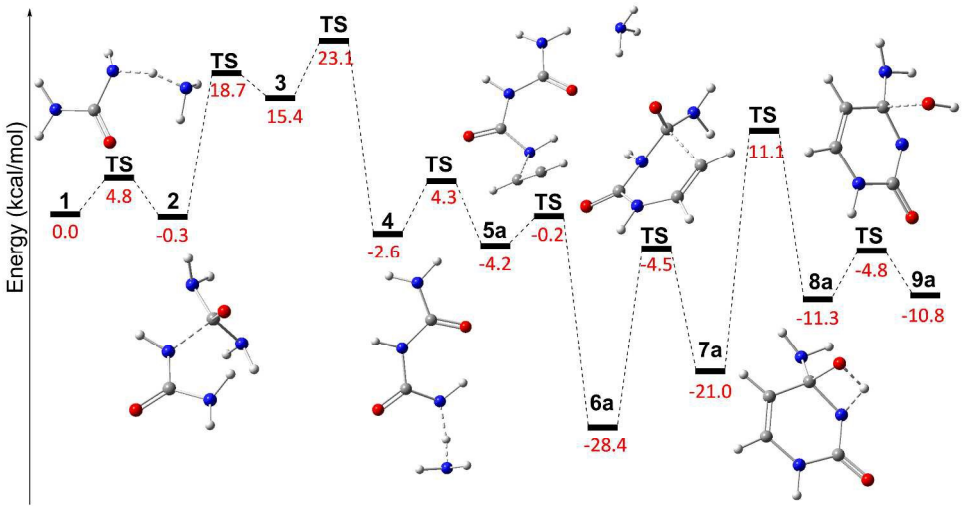

Potential energy surface for formation of cytosine from HCCH. Relative energies are given in kcal/mol were obtained from B3LYP/6-311G(d,p) + ZPE computations

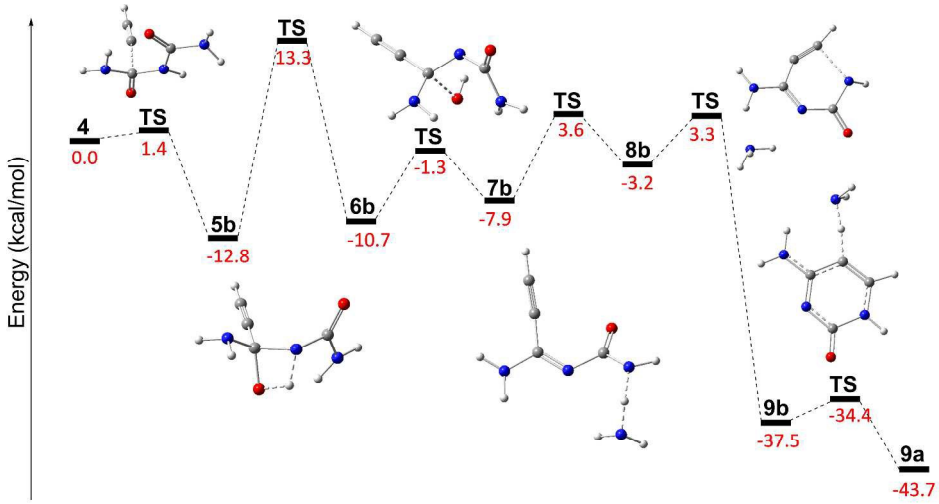

Figure 2. Potential energy surface for formation of cytosine from •CCH. Relative energies are given in kcal/mol were obtained from B3LYP/6-311G(d,p) + ZPE computations

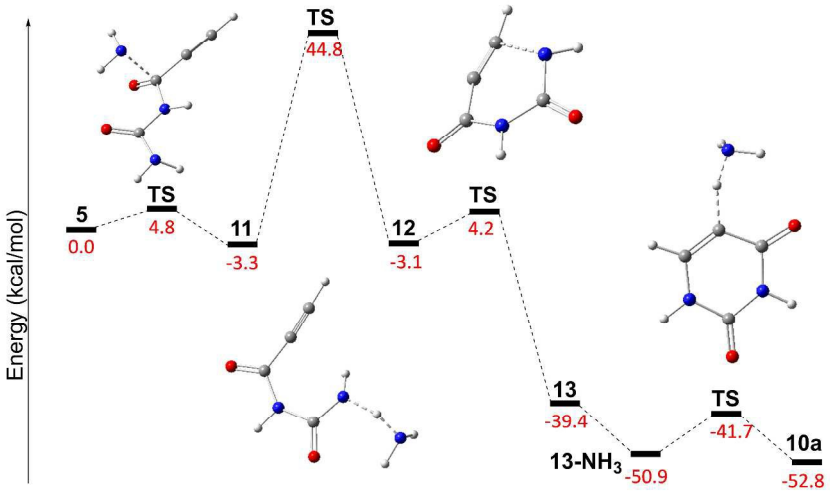

Figure 3. Potential energy surface for formation of uracil from •CCH. Relative energies are given in kcal/mol were obtained from B3LYP/6-311G(d,p) + ZPE computations

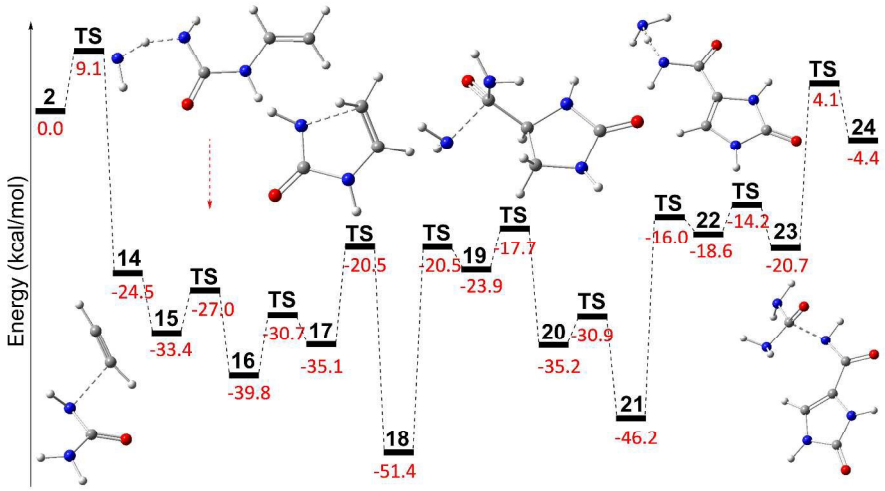

Figure 4. Potential energy surface for formation of intermediated 24

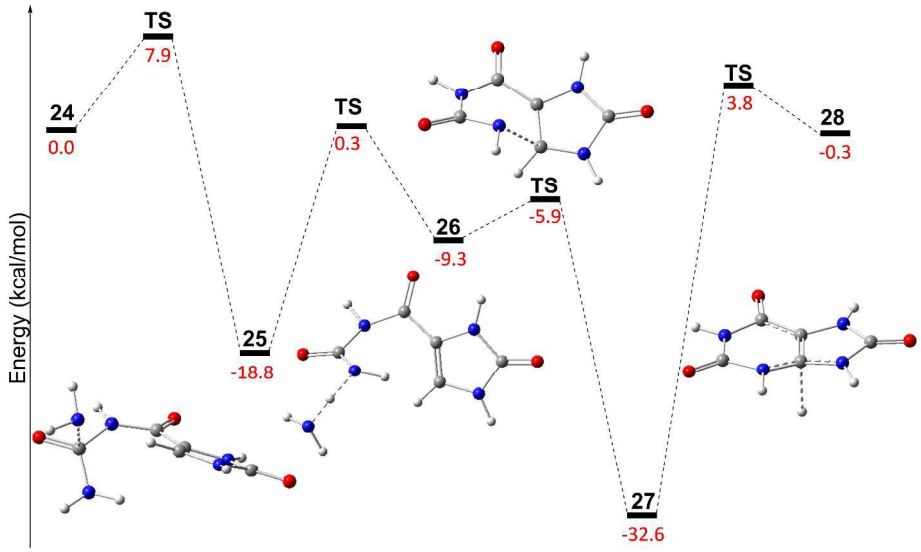

Figure 5. Potential energy surface for formation of uric acid. Relative energies are given in kcal/mol were obtained from B3LYP/6-311G(d,p) + ZPE computations

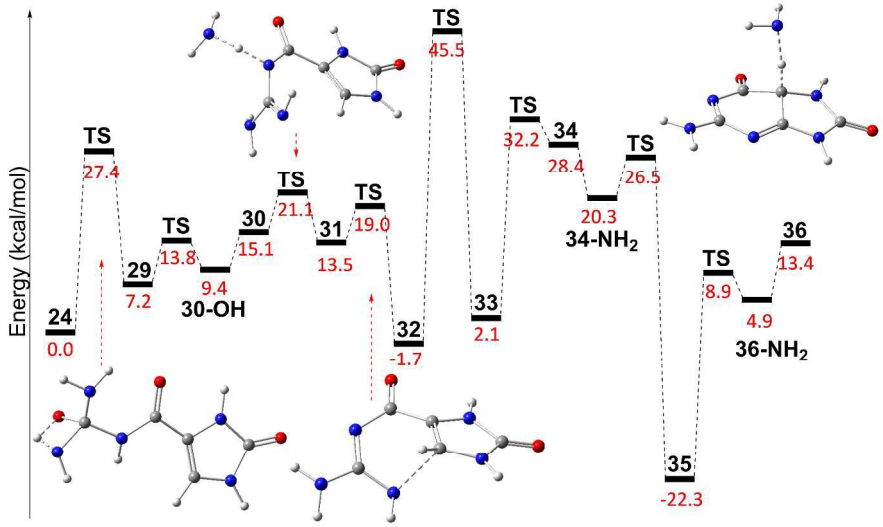

Figure 6. Potential energy surface for formation of 8-oxoguanine. Relative energies are given in kcal/mol were obtained from B3LYP/6-311G(d,p) + ZPE computations

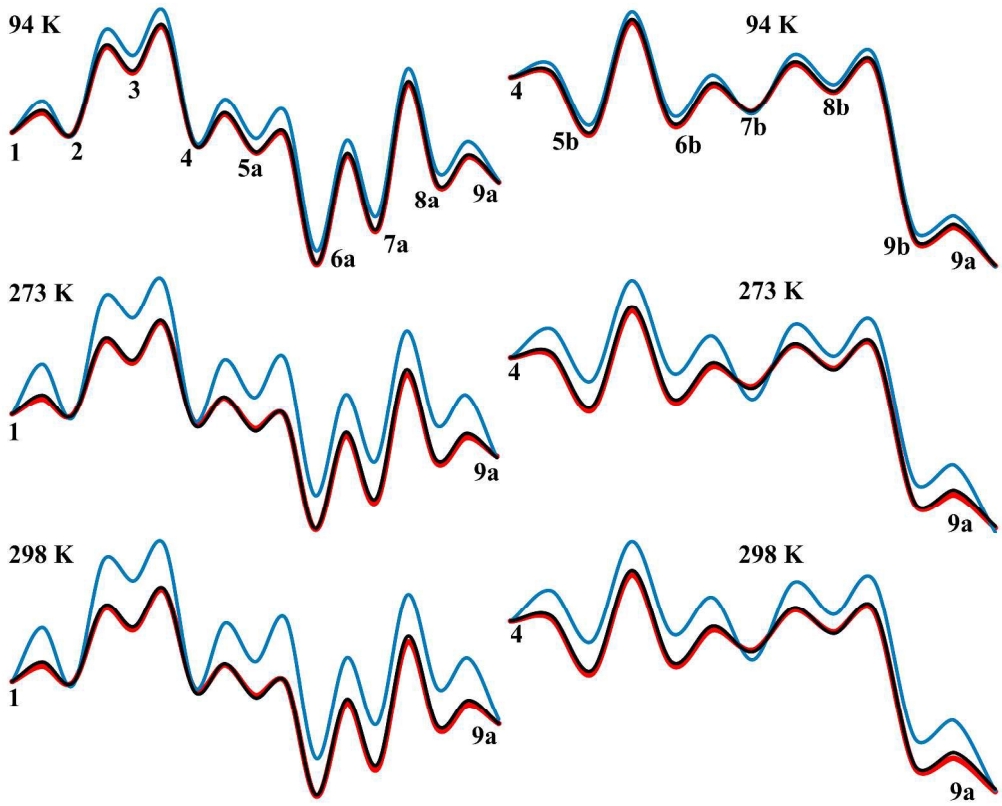

Figure 7. Energy, enthalpy and Gibbs free energy profiles (black, red, and blue respectively) of the HCCH and •CCH routes leading to the formation of cytosine (9a) from formamide at 94 K, 273 K and 298 K. Relative energies are given in kcal/mol were obtained from B3LYP/6-311G(d,p) + ZPE computations